Thin Solid Films xxx (2013) xxx–xxx

Contents lists available at ScienceDirect

Thin Solid Films

journal homepage: www.elsevier.com/locate/tsf

Confinement in single walled carbon nanotubes investigated by spectroscopic ellipsometry

Y. Battie [a,*], D. Jamon [b], J.S. Lauret [c], Q. Gu [d], M. Gicquel-Guézo [d], A. En Naciri [a], A. Loiseau [e]

[a] LCP-A2MC, Institut Jean Barriol, Université de Lorraine, 1 Bd Arago, 57070 Metz, France
[b] Université de Lyon, Université Jean Monnet, EA 3523, Laboratoire Télécom Claude Chappe, 25 rue du Dr Rémy Annino, 42000 Saint Etienne, France
[c] Laboratoire Aimé Cotton, UPR 3321, ENS Cachan, 94245 Cachan, France
[d] FOTON, UMR 6082, INSA, Avenue des Buttes de Coësmes, 35043 Rennes, France
[e] Laboratoire d'étude des microstructures, ONERA-CNRS UMR 104, 29 Av. de la Division Leclerc, 92322 Chatillon, France

ARTICLE INFO

Available online xxxx

Keywords:
Ellipsometry
Dielectric function
Carbon nanotube film
Confinement

ABSTRACT

Thick films of single walled carbon nanotubes (SWCNTs) with different diameter and chirality distributions are characterized by combining transmission electron microscopy and spectroscopic ellipsometry. The dependence of the dielectric function with the increase of the SWCNT diameter occurs with a drastic redshift of the S_{11}, S_{22} and M_{11} transition energies. The transfer integral parameter γ_0 of SWCNT is also evaluated and analyzed. We demonstrate that parts of the optical properties of SWCNTs are attributed to a one dimensional confinement effect.

1. Introduction

Single walled carbon nanotube (SWCNT) is a cylindrical nanostructure which can be viewed as a rolled up graphene sheet. Depending on its chirality, a SWCNT can be a metallic or a semiconducting material. Due to its one-dimensional structure, the density of states of SWCNT exhibits Van Hove singularities (VHS). Their optical properties are closely related to the transitions between VHS. Thus, SWCNTs have attractive optical properties aiming for the development of future photonic devices such as high-bit-rate all-optical signal regenerator [1,2] or high-repetition mode-locked lasers [3]. However, the dielectric function of SWCNT film is required to design and to produce such optoelectronic devices. As suggested by theoretical investigation based on ab-initio calculation [4] or tight binding approximation [5], the dielectric function of SWCNTs shows a strong dependence on their diameter and chirality. Ellipsometry is an indirect optical characterization tool which allows the measurement of the dielectric function of materials. Ellipsometry was recently exploited to characterize thin films with different SWCNT densities [6]. The authors of this paper argue that the interactions between SWCNTs reduce the electronic confinement. Ellipsometry was also used to determine the preferential orientation of anisotropic SWCNT network [7,8]. W. De Heer et al. [7] have analyzed their ellipsometric data by considering the SWCNT film as an effective anisotropic medium composed of a mixture of graphite and void. However, polarized reflectivity measurements [9] and tight binding calculation [5] suggest that the dielectric function of SWCNTs differs from the graphite one. Recently, we have demonstrated that the optical anisotropy of orientated SWCNT film is attributed to the relation between the polarisation and the selection rules [8]. To date, the relationship between the dielectric function of SWCNTs and their diameter remains unclear.

In this paper, the dielectric functions of conventional SWCNT thick films, extracted from ellipsometric measurements, are correlated to the diameter distributions deduced from transmission electron microscopy (TEM). In agreement with theoretical works [4,5], we demonstrate that the dielectric function of SWCNTs shows the signatures of the strong one-dimensional confinement.

2. Material preparation

Electrical arc discharge, high-pressure carbon monoxide (HiPco) and raw cobalt molybdenum catalyser (CoMoCat) SWCNTs, are purchased from Carbon Solution inc., Unidym and SouthWest Nanotechnologies, respectively. SWCNTs enriched in (6,5) chirality are sorted from raw CoMoCat SWCNTs using non-linear density gradient ultracentrifugation (DGU) process as described in [10]. The SWCNT aqueous suspensions are filtrated through nitrocellulose membranes with a 0.2 µm pore size as reported in [11]. The randomly orientated SWCNT films are then transferred on cleaned glass substrates by dissolving the nitrocellulose with acetone. The films are finally rinsed with distilled water and isopropanol and dried in air. In accordance with transmission spectroscopy measurements (not shown), these films are sufficiently thick to be completely opaque in the considered spectral range (0.6–5 eV). The thicknesses estimated by mechanical profilometry are closed to 500–600 nm.

* Corresponding author. Tel./fax: +33 3 87 54 70 57.
E-mail address: yann.battie@univ-lorraine.fr (Y. Battie).

0040-6090/$ – see front matter © 2013 Elsevier B.V. All rights reserved.
http://dx.doi.org/10.1016/j.tsf.2013.10.072

3. Experimental characterisation

Transmission electron microscopy (TEM) was performed with a Technai CM20 electron microscope operating at 200 kV. To allow TEM observations, SWCNT film fragments were stripped off from the substrate by scratching the samples with a razor blade and were deposited onto a carbon-coated copper grid. Reflection ellipsometric measurements were carried out on SWCNT films in the 0.6–5 eV spectral range with a phase modulator ellipsometer. The incidence angles are 60° and 70°. Ellipsometry measures the variation of light polarization after reflection upon a surface [12]. The ellipsometric parameters Ψ and Δ are expressed by the fundamental equation:

$$\rho = \frac{r_p}{r_s} = \tan\Psi e^{j\Delta} \tag{1}$$

where r_p and r_s are the reflection coefficients for the p and s polarisations respectively.

4. Results and discussion

Fig. 1 displays the TEM images of electrical arc discharge, HiPco, CoMoCat and (6,5) enriched SWCNTs. Due to the Van Der Waals force, carbon nanotubes are aggregated into bundles. The diameter distribution extracted from TEM images by a statistical analysis over more than fifty SWCNTs is also reported in Fig. 1. This reveals that the diameter follows a Gaussian distribution. The mean diameter can be extracted from the Gaussian distribution after a non-linear fit of the measured diameter distribution. The mean diameter of electrical arc discharge, HiPco, CoMoCat and (6,5) enriched SWCNTs is 1.3 nm ±0.12 nm, 0.95 nm ±0.09 nm, 0.75 nm ±0.08 nm and 0.75 nm ±0.08 nm, respectively. CoMoCat and (6,5) enriched SWCNTs have similar diameter distributions. This suggests that the change in the diameter distribution induced by the chirality sorting process is in the same order of magnitude of the TEM resolution.

Fig. 2 illustrates the Ψ and Δ ellipsometric angles measured at an angle of incidence of 70° on the four SWCNT films. Differences are clearly observed between each ellipsometric spectra. This suggests that the optical properties of SWCNT film depend on the nature SWCNT. To give a better quantitative analysis, the dielectric function must be extracted from ellipsometric spectra. Ellipsometry is an indirect characterisation tool which needs to establish an optical model to exploit the experimental data. In the considered spectral range, films are sufficiently opaque to consider them as semi-infinite isotropic substrates. The complex effective dielectric function ε was determined analytically from [12]:

$$\varepsilon(\omega) = \sin^2\theta_0\left(1+\frac{1-\rho(\omega)}{1+\rho(\omega)}\right)^2 \tan^2\theta_0 \tag{2}$$

where θ_0 is the angle of incidence and ω the photon energy.

Fig. 3 shows the real part ε_r and imaginary part ε_i of the complex dielectric function of SWCNT films. Same dielectric functions were also obtained from measurements recorded at an angle of incidence of 60° (not shown) confirming the isotropic behaviour of these films. This suggests that the surface roughness is sufficiently small to be neglected. Several bands can be clearly distinguished in the ε_r and ε_i spectra.

In accordance with the Kramers–Kronig relation [13], strong variations in ε_r occur when ε_i is maximized i.e. at the transition energies. In the considered spectral range, the dielectric functions are in the same order of magnitude for all SWCNT films. However, their shapes are completely different. The broad bands observed at 4 eV for raw and (6,5) enriched CoMoCat SWCNTs, 4.5 eV for HiPco and arc discharge SWCNTs come from the collective excitation of the π-plasmon bands [4,5]. Recent ab-initio calculation performed on isolated SWCNTs suggests that the position of the π-plasmon band is blueshifted towards the graphite one as the SWCNT diameter increases [4]. Graphite is an anisotropic structure characterized by an in-plane and an out of plane dielectric function. As mentioned by Jonhson et al. [14], the imaginary part of the ordinary dielectric function of graphite has a maximum at 4.5 eV, similar to position of the π-plasmon band of HiPco and arc discharge SWCNTs. Moreover, Park et al. [15] have argued that the position of the π-plasmon band depends on the SWCNT environment and especially the interaction between SWCNTs. In other words, the π-plasmon band is correlated to the concentration ratio between metallic and semiconducting SWCNTs [15]. As shown by Naumov et al. [16], CoMoCat contains more than 90% of semiconducting SWCNTs while HiPco and arc discharge SWCNTs contain statistically nearly 66% of semiconducting carbon nanotubes. As a consequence, similar positions of the π-plasmon band are expected for HiPco and arc discharge SWCNTs while a shift of the π-plasmon is awaited for CoMoCat SWCNT films.

Bands located at lower energies than 3.5 eV are associated to the transitions between the first S_{11} and second S_{22} pairs of VHS of semiconducting SWCNTs and the transition between the first pair M_{11} of VHS of

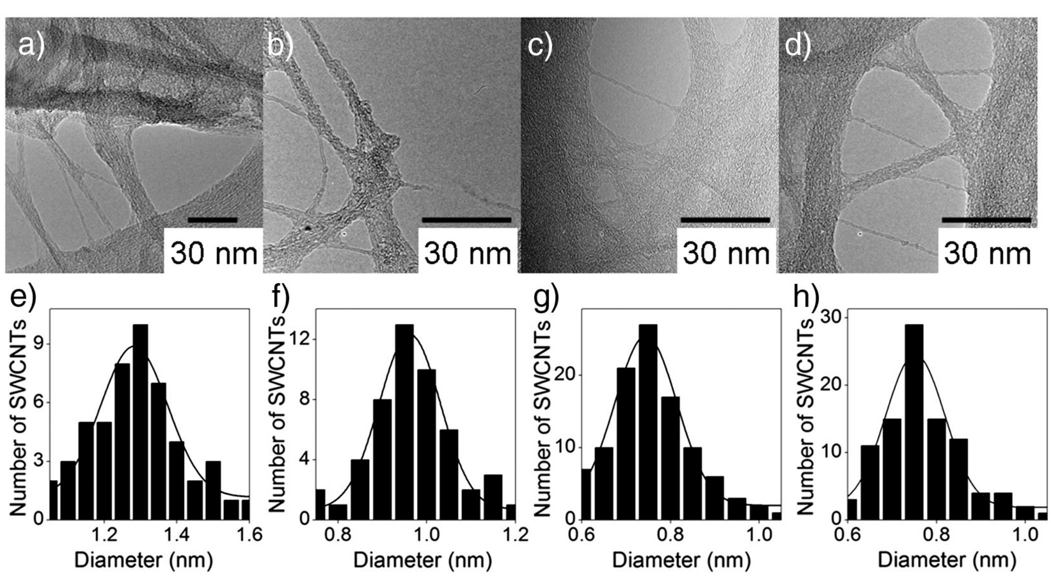

Fig. 1. (a)–(d) TEM pictures and (e)–(h) diameter distributions of (a)(e) arc discharge, (b)(f) HiPco, (c)(g) raw and (d)(h) (6,5) enriched CoMoCat SWCNTs.

Please cite this article as: Y. Battie, et al., Thin Solid Films (2013), http://dx.doi.org/10.1016/j.tsf.2013.10.072